energies

MDPI

Article

Load Optimization for Connected Modern Buildings Using Deep Hybrid Machine Learning in Island Mode

Seyed Morteza Moghimi [1,*], Thomas Aaron Gulliver [1,*], Ilamparithi Thirumarai Chelvan [1,†] and Hossen Teimoorinia [2,3,†]

[1] Department of Electrical and Computer Engineering, University of Victoria, P.O. Box 1700, STN CSC, Victoria, BC V8W 2Y2, Canada
[2] Department of Physics and Astronomy, University of Victoria, Victoria, BC V8P 5C2, Canada
[3] NRC Herzberg Astronomy and Astrophysics, 5071 West Saanich Road, Victoria, BC V9E 2E7, Canada
* Correspondence: seyedmortezamoghimi@uvic.ca (S.M.M.); agullive@ece.uvic.ca (T.A.G.)
† These authors contributed equally to this work.

Abstract: This paper examines Connected Smart Green Buildings (CSGBs) in Burnaby, BC, Canada, with a focus on townhouses with one to four bedrooms. The proposed model integrates sustainable materials and smart components such as recycled insulation, Photovoltaic (PV) solar panels, smart meters, and high-efficiency systems. These elements improve energy efficiency and promote sustainability. Operating in island mode, CSGBs can function independently of the grid, providing resilience during power outages and reducing reliance on external energy sources. Real data on electricity, gas, and water consumption are used to optimize load management under isolated conditions. Electric Vehicles (EVs) are also considered in the system. They serve as energy storage devices and, through Vehicle-to-Grid (V2G) technology, can supply power when needed. A hybrid Machine Learning (ML) model combining Long Short-Term Memory (LSTM) and a Convolutional Neural Network (CNN) is proposed to improve the performance. The metrics considered include accuracy, efficiency, emissions, and cost. The performance was compared with several well-known models including Linear Regression (LR), CNN, LSTM, Random Forest (RF), Gradient Boosting (GB), and hybrid LSTM–CNN, and the results show that the proposed model provides the best results. For a four-bedroom Connected Smart Green Townhouse (CSGT), the Mean Absolute Percentage Error (MAPE) is 4.43%, the Root Mean Square Error (RMSE) is 3.49 kWh, the Mean Absolute Error (MAE) is 3.06 kWh, and R^2 is 0.81. These results indicate that the proposed model provides robust load optimization, particularly in island mode, and highlight the potential of CSGBs for sustainable urban living.

Keywords: load optimization; Smart Green Buildings; island mode; hybrid Machine Learning

Citation: Moghimi, S.M.; Gulliver, T.A.; Thirumarai Chelvan, I.; Teimoornia, H. Load Optimization for Connected Modern Buildings Using Deep Hybrid Machine Learning in Island Mode. *Energies* **2025**, *17*, 6475. https://doi.org/10.3390/en17246475

Gerardo Maria Mauro

Received: 19 September 2024
Revised: 17 December 2024
Accepted: 19 December 2024
Published: 23 December 2024

1. Introduction

As urban areas grow, the demand for sustainable living solutions increases. Integrating Renewable Energy Sources (RESs) such as Photovoltaic (PV) systems and Electric Vehicles (EVs) into Smart Green Buildings (SGBs) can reduce emissions and improve load efficiency. However, optimizing energy usage in these dynamic environments remains a challenge [1]. In 2019, buildings accounted for 32% of primary energy use in the US, with global consumption projected to rise by 1.3% annually until 2050 [1]. Space heating, cooling, and lighting consume almost half of this energy [2], making load prediction and optimization in SGBs essential for reducing energy waste, costs, and environmental impact [3,4].

Machine Learning (ML) techniques have been considered to predict and optimize building energy consumption [5]. Hybrid models combining Long Short-Term Memory (LSTM) and Convolutional Neural Networks (CNNs) have been shown to improve prediction accuracy by capturing both temporal and spatial dependencies in energy data [6,7]. These models reduce energy costs and emissions, which contribute to building resilience.

Hybrid ML models such as Random Forest–Extreme Gradient Boosting–Linear Regression (RF–XGBoost–LR) have been shown to improve real-time prediction accuracy in Smart Buildings (SBs) and Smart Grids (SGs) [8–10]. The integration of distributed energy resources has been considered to optimize local energy generation and consumption to improve cost-effectiveness and flexibility [11].

To date, there has been limited research on island mode (off-grid) operation in residential buildings [12–14]. This study fills this gap by evaluating ML models for Connected Smart Green Townhouses (CSGTs) in Burnaby, British Columbia (BC), Canada, with a focus on island mode operation. Performance indicators such as energy efficiency, cost, emissions, and prediction accuracy are employed to support sustainable building operations [15]. A hybrid LSTM–CNN model is introduced to predict load consumption and optimize parameters such as Heating, Ventilation, and Air Conditioning (HVAC), lighting, and electricity use. The results demonstrate significant cost savings, emission reductions, and improved load efficiency and indicate that connected SGBs operating in island mode can contribute to sustainable urban development.

The remainder of this paper is organized as follows. Section 2 introduces energy demand prediction for CSGTs in island mode, including performance, cost, and emissions. Section 3 outlines the proposed ML model, while Section 4 presents the performance results. Finally, Section 5 summarizes the paper and discusses the implications for sustainable urban living.

2. SGT Modeling

The design and modeling of SGBs play a critical role in reducing Greenhouse Gas (GHG) emissions and supporting climate goals. These buildings incorporate advanced technologies, such as energy-efficient HVAC systems and Photovoltaic (PV) solar panels, to improve load efficiency, resulting in substantial energy savings and cost reductions. As one of the strategies toward a sustainable future, SGBs contribute to environmentally friendly urban development. This section outlines the modeling of Connected SGTs (CSGTs), focusing on the integration of sustainable technologies to optimize performance.

Canada has significant energy and climate challenges but there is a lack of research, particularly regarding the impact on load consumption and energy optimization in SGBs [16–18]. This is addressed here with a focus on the geographic and climatic conditions in Burnaby, BC. An understanding of these factors is crucial for designing SGTs tailored to environmental conditions. This research offers valuable insights into the challenges and opportunities for CSGTs in Burnaby, advancing sustainable building practices [19].

The daylight hours in a year in Burnaby exceed the sunshine hours. Daylight refers to the total hours of light each day, while sunshine reflects the availability of direct sunlight, which affects solar energy harvesting. The longest daylight hours (16.02) occur in June, while the shortest hours (8.03) occur in December. This variation indicates higher solar energy potential in summer and reduced availability in winter. Heating Degree Days (HDDs) are also important for understanding climate and designing efficient heating systems for SGTs. The HDD in Burnaby is approximately 3000, which indicates moderate heating demand. This helps guide the optimal sizing and design of heating systems to meet local needs [20].

2.1. SGT Formulation

This paper considers the characteristic home described in [21–23] to develop an SGT model. The base model is a two-story townhouse (2140 sq ft) located in Burnaby. It was built in 1995 and underwent significant renovations in 2007–2008 [21]. Major renovations typically occur every 15–20 years, depending on the condition of the building, regulatory changes, and advances in sustainable technology. The home is oriented southward to maximize solar energy utilization.

LEED certification and Canada Green Building Council (CGBC) standards are considered to reduce emissions and improve load efficiency [21]. SGTs are designed to operate solely on electricity to minimize on-site emissions, supported by PV systems with the goal of net-zero energy [24]. During sunny months, surplus electricity can be exported to neighboring buildings, offsetting consumption during colder months.

Sustainable materials include bamboo flooring, recycled wood, PV panels, LED lighting, and high-efficiency heat pumps. These materials are widely used in sustainable construction projects [25–27]. They must adhere to applicable local and international building codes, including sustainability and safety requirements [28–30]. Heat pumps and modern air conditioning systems provide energy-efficient year-round temperature control [31,32]. Heat pumps supply both heating and cooling and are more energy-efficient than traditional HVAC systems. Smart air conditioners optimize cooling by automatically turning off when not required, reducing energy consumption.

This work employs sustainable materials for SGTs in Canada [33]. Windows with a thermal resistance of R6 are used to reduce heat transfer and improve insulation, helping to maintain indoor comfort and lower heating and cooling loads [33]. This high thermal resistance is especially beneficial for energy efficiency in colder climates. The R2000 standard for energy-efficient housing in Canada is also employed [34]. It incorporates advanced insulation and ventilation systems. Table 1 gives the components and materials used in SGTs as well as the technologies and features that contribute to sustainable buildings.

The townhouse sizes and layouts are optimized for different family needs and energy usage. The one-bedroom (one-Bd) SGT is designed for a young couple, focusing on compact living with minimal energy consumption. The two-Bd SGT is suitable for a couple with one young child, providing extra space while being energy efficient. The three-Bd SGT caters to a family with two teenage children, prioritizing efficient zoning and energy distribution. The four-Bd SGT is designed for a family of five, incorporating advanced energy systems to accommodate higher energy demands.

Table 2 gives the specifications for hot water tank, HVAC, and PV capacity in SGTs (island mode). PV system capacity refers to the peak output under ideal sunlight conditions (i.e., under standard test conditions) and does not account for daily or monthly output variations due to location-specific factors such as weather, shading, or panel orientation. Operating in island mode increases resilience and reliability to allow SGBs to function independently of the grid and ensure an uninterrupted energy supply during outages. This maximizes the use of locally generated renewable energy such as from PV panels, and EV batteries for storage, promoting energy independence and decentralized resource management. Integrating island mode with advanced technologies like Vehicle-to-Grid (V2G) systems and Machine Learning (ML) models provides an innovative solution to modern energy challenges. These models improve load prediction to optimize energy resources and support sustainability so SGBs can be an environmentally friendly urban solution.

Figure 1 shows the proposed SGT and its components in island mode. These include PV panels, energy-efficient HVAC (e.g., heat pump), and a high-performance hot water tank [35]. These systems are modeled in OpenStudio to evaluate energy performance. Data are collected using meters that measure electricity, water, and gas consumption. These data are processed and stored on a central server. A WiFi access point provides communication between the server and devices, while cloud storage supports remote access and long-term data storage. This setup enables efficient resource management and informed decision-making [16–18].

Table 3 presents the PV panel parameters for the SGTs, including roof area, panel capacity, energy output, payback period, and cell efficiency, as well as the battery system specifications when operating in island mode. These values were obtained using the results in [36,37]. This shows that the roof area, panel capacity, and estimated annual energy output increase with the number of bedrooms. Larger townhouses have more roof area, supporting higher-capacity panels. The energy saved annually is the same as the PV system output, reflecting efficient utilization. Battery storage is specified to provide energy autonomy for

1.5 days. This allows for short-term off-grid operation. The payback period is the time required to recover installation and other costs from the energy savings and is given by

$$\text{Payback Period (years)} = \frac{\text{Total Installation Cost}}{\text{Annual Energy Savings}} \quad (1)$$

where Total Installation Cost includes all PV system expenses, including panels, inverters, batteries, wiring, and labor. The Annual Energy Savings is the yearly monetary value of energy saved, calculated by multiplying the PV system energy generated (kWh) by the local electricity rate (CAD/kWh). After the payback period, the system provides nearly free energy, aside from maintenance. The SGTs use lithium-ion batteries for energy storage. The capacities range from 9.0 kWh for a 1-Bd unit to 18.0 kWh for a 4-Bd unit, each supporting 1.5 days of off-grid operation. Larger SGTs produce more energy but need more storage and have longer payback periods.

Table 1. Materials and smart technologies used in SGTs.

Material/Technology	Description
Air Conditioner	High-efficiency cooling system.
Bamboo Flooring	Renewable, durable, and eco-friendly.
Connected Appliances	Internet connection for remote monitoring and control.
Cork Wall Insulation	Renewable, lightweight, and excellent insulation.
Envelope and Structural Mass	Improved insulation and thermal mass for load efficiency.
EV Charger	Electric vehicle charging station.
Heat Pump	Energy-efficient heating and cooling.
Hot Water Tank	Utilizes recycled materials for thermal insulation.
Light Emitting Diode (LED) Lighting	Energy-efficient and long-lasting.
Low Volatile Organic Compound (VOC) Paint	Reduces indoor air pollution.
PV Panels	RES to reduce electricity costs.
R6 Windows	High-performance windows to reduce heat loss and improve load efficiency.
Rainwater Harvesting System	Collects rainwater for irrigation.
Reclaimed Wood	Recycled, unique aesthetic, and reduces deforestation.
Recycled Glass Countertops	Eco-friendly, durable, and visually appealing.
Recycled Insulation Materials	Eco-friendly materials for thermal insulation.
Recycled Wood	High strength, recyclable, and long-lasting.
Smart Home (SH) Hub	Connect and manage smart devices, facilitating remote monitoring.
Smart Meters	Monitor and optimize load consumption.
Smart Plugs	Enable remote control and energy monitoring.
Smart Thermostat	Programmable and energy-efficient temperature control.
EVs such as a Tesla 3	Environmentally friendly transportation with zero emissions.

Table 2. Specifications for hot water tank, HVAC, and PV capacity in SGTs (island mode).

Townhouse Type	Hot Water Tank Capacity (Gallons)	Daily Hot Water Consumption (Gallons/Day)	HVAC System Capacity (Tons)	PV System Capacity (kW)
Base	20.1	45.3	1.1	2.2
One-Bd	30.3	55.6	1.3	2.8
Two-Bd	39.1	75.2	1.9	3.5
Three-Bd	48.9	95.2	2.5	4.2
Four-Bd	60.3	110.1	2.8	5.4

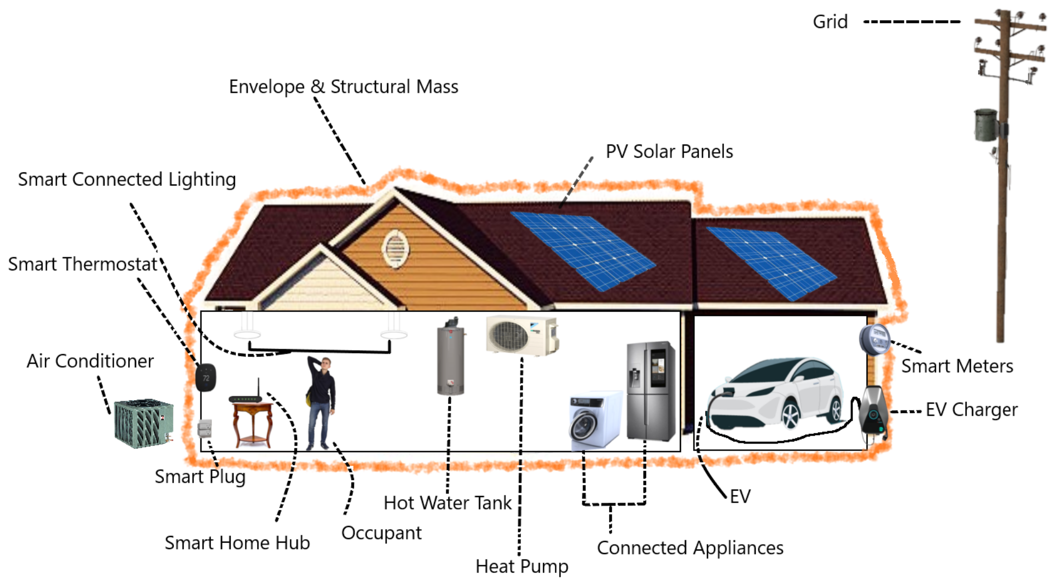

Figure 1. The SGT components in island mode.

Table 3. PV panel and battery storage specifications for SGTs in island mode.

Parameter	1-Bd SGT	2-Bd SGT	3-Bd SGT	4-Bd SGT
Roof Area (sq ft)	764	1080	1543	1736
Panel Capacity per Unit (W)	300	400	500	600
Total System Capacity (kW)	2.6	3.2	3.8	4.5
Estimated Annual Energy Output (kWh)	3070	3840	4610	5380
Energy Saved Annually (kWh)	3070	3840	4610	5380
PV Cell Area (sq ft)	193	251	309	361
Battery Storage (kWh)	9.0	12.0	15.0	18.0
Autonomy Period (Days)	1.5	1.5	1.5	1.5

2.2. CSGT Formulation

Connecting residential buildings significantly reduces energy consumption and costs [38]. For SGTs, connecting units improves efficiency and enables better energy management. Linking modern residential townhouses is similar to Micro-Grids (MGs) [39,40]. Here, CSGTs in island mode are examined to assess their performance and determine the benefits for load optimization and sustainability.

Key components of connected townhouses are connected water systems [21,41] and party walls [42,43]. Party walls are shared walls between neighboring properties and are common in townhouses and semi-detached homes. They serve as boundaries and are jointly owned and maintained. Party wall agreements specify structural maintenance, repairs, alterations, and dispute resolution [42,43]. In CSGTs, party walls provide structural integrity, noise reduction, and fire safety. Connected water systems are important for building performance, occupant comfort, and sustainability. District cooling provides chilled water across multiple buildings. This work examines district cooling performance, load patterns, temperature management, and efficiency [41]. It also considers how building operations impact cooling infrastructure effectiveness.

The CGST performance expressions are based on [44,45]. The heat transfer is given by

$$Q = k \cdot A \cdot \frac{\Delta T}{d} \tag{2}$$

where Q is the heat transfer rate, k is the thermal conductivity of the wall material, A is the surface area of the wall, ΔT is the temperature difference across the wall, and d is the thickness of the wall. This describes conductive heat transfer, where thermal energy moves through a solid material. It is proportional to the thermal conductivity of the material and the cross-sectional area through which the heat moves. The goal is to minimize heat loss or gain and optimize energy use in CGSTs.

Continuity is very important in fluid dynamics and is given by

$$\frac{d(\rho A)}{dt} = \dot{m}_{\text{in}} - \dot{m}_{\text{out}} \tag{3}$$

so the rate of change of mass (ρA) within a volume is equal to the difference between the mass flow rate entering $(\dot{m}_{\text{in}})$ and leaving $(\dot{m}_{\text{out}})$ the system. This is applied to fluid systems within CSGTs such as HVAC, plumbing, and other fluid transport mechanisms such as rainwater harvesting systems.

The load consumption is

$$C = \sum_{i=1}^{n} C_i \tag{4}$$

The goal is to minimize C which is the sum of the load consumptions C_i of different components, systems, or time periods, while maintaining comfortable temperature levels and adequate flow rates. The building energy balance is

$$\text{Energy In} - \text{Energy Out} = \text{Energy Storage} \tag{5}$$

where Energy In includes total load consumption. Total load consumption includes electrical consumption (e.g., lighting and HVAC), gas consumption, and water consumption. Energy Out includes heat loss, heat gain, total load consumption output, and PV panel output. In island mode, buildings operate independently from the grid, so PV output is considered an output when it is stored in batteries and used to meet building energy needs. The PV output is a source of energy that contributes to building self-sufficiency. Energy Storage is changes in internal and external energy storage within the building.

Renewable Energy Integration (REI) refers to the incorporation of RESs into a building energy system in island mode and is given by

$$\text{REI} = \frac{\text{Renewable Energy Used}}{\text{Total Energy Consumption}} \times 100\% \tag{6}$$

where Renewable Energy Used is the amount of energy derived from RESs like PV panels and Total Energy Consumption is the total energy consumed by the building. It includes electricity consumption (e.g., lighting and HVAC), gas consumption, and water consumption.

The Smart Technology Utilization Index (STUI) is used to quantify the effectiveness and efficiency of smart technology implementation in a building. It is expressed as

$$\text{STUI} = \frac{\text{Number of Smart Devices}}{\text{Total Devices}} \times 100\% \tag{7}$$

where Number of Smart Devices is the total number of smart devices used in the building and Total Devices is the total number of devices in the building.

SGTs range from base to 4-Bd units. The base and 1-Bd units have 1 bathroom, the 2-Bd unit has 2 bathrooms, and the 3-Bd and 4-Bd units have 3 bathrooms. Kitchen sizes vary from 60 sq ft (base) to 150 sq ft (4-Bd). Dining rooms range from 40 sq ft (base) to 120 sq ft (4-Bd). Living rooms range from 120 sq ft (1-Bd) to 250 sq ft (4-Bd). Entrance spaces are from 30 sq ft (base) to 90 sq ft (4-Bd). Deck sizes are 40 sq ft to 150 sq ft. The first bedroom is 100 sq ft in the base unit and 120 sq ft in the others. The 2-Bd to 4-Bd units have a second bedroom (120 sq ft) and a master bedroom (150–250 sq ft). There is a second master bedroom (150–200 sq ft) in the 3-Bd and 4-Bd units. Garage space is available only in the 3-Bd (154.1 sq ft) and 4-Bd (173.8 sq ft) units. The base unit is 680.0 sq ft while the 4-Bd unit is 1735.9 sq ft. Heights are 8.0 ft (base) and 16.5 ft (other units). The base unit has a 20-gallon hot water tank, 1.0 ton HVAC system, and 1.80 kW PV panels. These capacities increase to a 60.3-gallon hot water tank, 3.1 ton HVAC system, and 4.48 kW PV panels in the 4-Bd unit.

2.3. Performance Metrics

This section presents the metrics to assess building efficiency, accuracy, performance, emissions, and costs. The Total Energy Use Intensity (TEUI) is

$$\text{TEUI} = \frac{\text{Total Energy Consumption}}{\text{Total Building Area}} \tag{8}$$

where Total Energy Consumption is the sum of all forms of energy consumption within the building in kWh and Total Building Area is the total floor area of the building in sq ft. The Total Energy Demand Intensity (TEDI) is

$$\text{TEDI} = \frac{\text{Total Energy Demand}}{\text{Total Building Area}} \tag{9}$$

where Total Energy Demand is the sum of the peak energy demand from all sources within the building in kW.

The Control Efficiency Index (CEI) is used to quantify the effectiveness of control systems in achieving desired outcomes within the building and is given by

$$\text{CEI} = \frac{\text{Actual Energy Usage (AEU)}}{\text{Optimal Energy Usage (OEU)}} \times 100\% \tag{10}$$

where Actual Energy Usage (AEU) is the actual energy consumed by the building and Optimal Energy Usage (OEU) is the energy usage under ideal conditions. This metric is crucial for building energy management as it helps to identify inefficiencies in control strategies and provides a basis for optimizing performance.

The Indoor Air Quality index (IAQ) is a measure of indoor air quality. It is used to quantify the quality of indoor air within the building and is

$$\text{IAQ} = \frac{\text{IAQ Measurement}}{\text{Maximum Acceptable IAQ}} \times 100\% \tag{11}$$

where Maximum Acceptable IAQ is the maximum acceptable level of indoor air quality. It evaluates various indoor air quality parameters such as Carbon Dioxide (CO_2) levels, Volatile Organic Compounds (VOCs), Carbon Monoxide (CO), and Ozone (O_3) [46].

Waste Recycling Rate (WRR) is used to quantify the proportion of waste materials that are recycled or diverted from landfills and is given by

$$\text{WRR} = \frac{\text{Weight of Recycled Waste}}{\text{Total Weight of Waste}} \times 100\% \tag{12}$$

where Weight of Recycled Waste is the total weight of the waste materials recycled and Total Weight of Waste is the total weight of the waste materials generated. This reflects the effectiveness of building waste management, with higher values indicating better recycling performance. It is used to identify areas within the building where waste recycling practices may need to be improved such as common areas and kitchens. Material Recycling Percentage (MRP) is used to assess the sustainability performance of SGBs and is given by

$$\text{MRP} = \frac{\text{Weight of Recycled Materials (WRM)}}{\text{Total Weight of Materials Used (TWMU)}} \times 100\% \tag{13}$$

where WRM is the total weight of the materials recycled and TWMU is the total weight of the materials used. A building with an average MRP of 75% is more likely to achieve green certification, reflecting a commitment to sustainability.

The water efficiency is

$$\text{Water Efficiency} = \frac{\text{Water Saved}}{\text{Total Water Used}} \times 100\% \tag{14}$$

It reflects the effectiveness of water-saving measures like low-flow fixtures and rainwater harvesting. The Electrical Consumption Efficiency (ECE) is

$$\text{ECE} = \frac{\text{Total Useful Electrical Output}}{\text{Total Electrical Input}} \times 100\% \tag{15}$$

A higher ECE means that more input electricity is converted into useful energy. The Gas Consumption Efficiency (GCE) is

$$\text{GCE} = \frac{\text{Total Useful Heat Output From Gas}}{\text{Total Gas Input}} \times 100\% \tag{16}$$

It measures the efficiency of gas used for heating.

The insulation R-value measures thermal resistance and is given by

$$\text{R} = \frac{d}{k} \tag{17}$$

A higher value indicates better insulation, which improves building efficiency [35]. Important R-values include exterior walls (R-30, in $\text{ft}^2{\cdot}{}^\circ\text{F}{\cdot}\text{h/BTU}$), windows (R-5, triple-pane with low-emissivity coatings), roof/ceiling (R-50, for high insulation), and floor/slab (R-20, to reduce heat loss through the foundation). OpenStudio provides detailed thermal values based on the specified materials and their properties.

TEUI and TEDI quantify load consumption and efficiency to help reduce waste and optimize energy use [47]. GHGI gives the carbon footprint and is expressed as

$$\text{GHGI} = \frac{\text{Total Greenhouse Gas Emissions}}{\text{Building Floor Area}} \tag{18}$$

Compliance with TEUI, TEDI, and GHGI standards is crucial, as it ensures sustainability and thus building marketability to investors. High TEUI, TEDI, and GHGI ratings signify superior efficiency, making buildings more competitive. Economic viability [48] considers cost savings, Return on Investment (ROI), and cost-benefit ratios. These support informed decision-making for load efficiency to align with both regulatory and investment goals.

The Total Energy Consumption is

$$\text{Total Energy Consumption} = \text{Energy from Storage} + \text{Energy from Renewables} \tag{19}$$

where Energy from Storage is the energy supplied by the battery system and Energy from Renewables is the energy generated by local renewable sources, such as PV systems. This represents the energy used for building operation in island mode. It should be sufficient to ensure continuous function when the building is disconnected from the grid. The cost of energy is

$$\text{Cost of Energy} = \text{Total Energy Consumption} \times \text{Unit Cost} \tag{20}$$

where Total Energy Consumption is the total amount of energy consumed by the building and Unit Cost is the unit cost of the energy consumed. The cost savings are

$$\text{Cost Savings} = \text{Cost Before} - \text{Cost After} \tag{21}$$

where Cost Before is the total cost before implementing load efficiency initiatives and Cost After is the reduced cost after implementing load efficiency measures. This provides the financial savings by comparing costs before and after load efficiency measures are implemented.

The ROI is

$$\text{ROI} = \frac{\text{Net Savings}}{\text{Initial Investment}} \times 100\% \tag{22}$$

where Net Savings is the total savings from load efficiency measures and Initial Investment is the cost of implementing these measures. The net benefit is

$$\text{Net Benefit} = \text{Total Savings} - \text{Total Costs} \tag{23}$$

where Total Savings is the savings from load efficiency measures and Total Costs are the expenses for implementing and maintaining them. This provides the overall financial benefit.

The HVAC metric is defined as

$$\text{HVAC Metric} = \frac{1}{n}\sum_{i=1}^{n}\left(\frac{X_i - X_{\text{min},i}}{X_{\text{max},i} - X_{\text{min},i}}\right) \tag{24}$$

where X_i is the ith parameter value, $X_{\text{max},i}$ and $X_{\text{min},i}$ are the corresponding maximum and minimum values, and n is the number of parameters. The parameters included in this metric are heat transfer efficiency, fluid dynamics efficiency, building energy balance, TEUI, TEDI, cooling energy consumption, and IAQ.

In island mode, energy storage, backup power, load management, and resilience must be evaluated to reflect the operational constraints of off-grid systems. The charging and discharging of the battery is modeled by the State of Charge (SOC)

$$\text{SOC}(t) = \text{SOC}(t-1) + \frac{\text{P-charge}(t) \cdot \eta_{\text{charge}} - \text{P-discharge}(t)}{\text{E}_{\text{max}}} \tag{25}$$

where $\text{SOC}(t)$ is the battery charge at time t, $\text{P-charge}(t)$ and $\text{P-discharge}(t)$ are the corresponding charging and discharging power, η_{charge} is the charging efficiency, and E_{max} is the maximum energy capacity. The energy balance for the storage system in island mode is

$$\text{E}_{\text{storage}}(t) = \text{E}_{\text{storage}}(t-1) + \text{P}_{\text{PV}}(t) + \text{P}_{\text{backup}}(t) - \text{P}_{\text{load}}(t) - \text{P}_{\text{storage}}(t) \tag{26}$$

where $\text{E}_{\text{storage}}(t)$ is the stored energy at time t, $\text{P}_{\text{PV}}(t)$ is the PV system power, $\text{P}_{\text{backup}}(t)$ is the backup power, $\text{P}_{\text{load}}(t)$ is the building load, and $\text{P}_{\text{storage}}(t)$ is the power used for storage operations. The backup efficiency is

$$\text{Backup Efficiency} = \frac{\text{Total Backup Power Output}}{\text{Total Backup Power Input} + \text{Energy from Storage}} \times 100\% \tag{27}$$

where Total Backup Power Output is the useful backup power, Total Backup Power Input is the total energy consumed by the backup system, and Energy from Storage is the energy drawn from the storage system. Battery degradation over time is modeled by

$$\text{Capacity}(t) = \text{Capacity}(t-1) \cdot (1 - \text{Degradation Rate}) - \text{Capacity Loss Due to Usage} \tag{28}$$

where $\text{Capacity}(t)$ is the remaining battery capacity at time t, Degradation Rate is the loss rate per cycle, and Capacity Loss Due to Usage accounts for additional loss due to use.

Table 4 gives the water system and party wall results for CSGTs in island mode. This shows that the PV system output ranges from 7.2 to 12.2 kWh/day, indicating reliable energy generation. HVAC usage is lower, reflecting efficient energy management. Daily hot water use is consistent across the townhouse sizes, demonstrating good system capability. Energy savings from shared walls range from 8.5% to 18.3% and indicate the impact of connected infrastructure on reducing load. Compared to SGTs in island mode, CSGTs outperform in PV panel output, energy savings, and HVAC efficiency. Thus, connected SGTs are more resilient and sustainable during off-grid operation.

Table 4. Outcomes related to water systems and party walls in the CSGTs in island mode.

Parameter	1-Bd	2-Bd	3-Bd	4-Bd
Daily Hot Water Usage (Gal/Day)	55.1	80.7	105.3	125.2
Energy Savings from Shared Walls (%)	8.5	12.1	15.2	18.3
PV Panel Output (kWh/Day)	7.2	8.9	10.5	12.2
HVAC System Usage (Tons/Day)	1.2	1.7	2.3	2.6

Table 5 gives the monthly energy performance for SGTs and CSGTs in island mode without an ML model. These results were generated using Python 3.11.15 and EnergyPlus 23.1 with the pyenergyplus library. The building model was created in OpenStudio 3.8.0 with .osm files converted to EnergyPlus input files (.idf). Table 5 shows that CSGTs have 5% to 7% lower energy consumption per square foot due to energy sharing and advanced management. The TEUI is improved by 10% and the TEDI is better by up to 12%. The HVAC and water efficiency are 2% to 4% better and CO_2 emissions per kWh are 3% to 5% lower. Better insulation and renewable energy use reduce heating and cooling loads, lowering costs by 2% to 4% and increasing ROI by 5% to 7%. These results illustrate CSGT sustainability, cost-effectiveness, and energy efficiency, making them a superior choice for modern buildings.

Table 5. Monthly energy performance for SGTs and CSGTs in island mode without an ML model.

Parameter	Disconnected				Connected				Acceptance Range
	1-Bd	2-Bd	3-Bd	4-Bd	1-Bd	2-Bd	3-Bd	4-Bd	
Efficiency									
Heat Transfer (%)	84.1	85.2	86.3	87.4	85.0	86.5	87.8	89.1	80–90
Fluid Dynamics (%)	78.2	79.6	80.5	81.6	79.3	80.8	82.0	83.5	75–85
Total Energy Consumption (kWh/sq ft)	0.79	0.73	0.71	0.68	0.76	0.72	0.69	0.67	0.65–0.80
Building Energy Balance (%)	90.2	91.3	92.4	93.5	91.5	92.6	93.7	94.8	85–95
TEUI (kWh/sq ft)	0.81	0.79	0.78	0.76	0.69	0.66	0.64	0.61	0.60–0.80
TEDI (kWh/sq ft)	0.45	0.44	0.41	0.39	0.41	0.38	0.37	0.36	0.35–0.50
HVAC Metric (%)	90.2	91.0	91.8	92.6	91.2	92.1	93.0	93.8	85–95
Water Efficiency (%)	79.5	79.9	80.7	81.3	80.5	80.9	81.6	82.2	75–85
ECE (%)	95.1	95.7	96.3	96.9	96.0	96.5	97.1	97.7	90–98
GCE (%)	87.3	88.1	88.9	89.7	88.5	89.3	90.1	90.9	85–95
Insulation R-Value (%)	24.0	24.3	24.6	24.9	24.7	25.0	25.4	25.7	20–30
Cost Savings (CAD)	380.5	410.6	440.7	470.8	396.0	426.8	457.4	488.2	-
Performance									
RE Integration (%)	30.5	35.1	39.7	44.3	31.2	36.0	40.8	45.6	30–50
STUI (%)	92.5	93.4	94.3	95.2	93.7	94.5	95.4	96.2	90–97
Cooling Energy Consumption (kWh/sq ft)	0.28	0.26	0.25	0.23	0.23	0.22	0.21	0.21	0.20–0.30
CEI (%)	86.2	87.1	88.0	88.9	87.5	88.4	89.3	90.2	85–95
WRR (%)	67.4	69.2	71.0	72.8	68.7	70.6	72.4	74.3	65–75
IAQ (%)	89.0	89.9	90.8	91.7	90.2	91.1	92.0	92.9	85–95
MRP (%)	73.1	73.9	74.7	75.5	74.3	75.1	76.0	76.8	70–80
Energy Storage									
Battery Charging Efficiency (%)	-	-	-	-	89.31	91.25	92.32	92.87	85–95
Battery Discharging Efficiency (%)	-	-	-	-	89.52	90.64	90.89	92.03	85–95
Energy Storage Capacity (kWh)	-	-	-	-	53.15	61.42	72.12	83.21	50–80
Backup Power Duration (hours)	-	-	-	-	4.23	4.95	6.12	7.31	4–8
Emissions									
GHGI ($kgCO_2/kWh$)	0.52	0.49	0.47	0.43	0.50	0.47	0.45	0.41	0.40–0.55

Table 5. *Cont.*

Parameter	Disconnected				Connected				Acceptance Range
	1-Bd	2-Bd	3-Bd	4-Bd	1-Bd	2-Bd	3-Bd	4-Bd	
Cost									
Cost of Energy (CAD)	550.5	620.8	690.2	761.7	538.0	607.8	677.2	748.5	-
ROI (%)	16.2	17.3	18.4	19.5	17.0	18.1	19.3	20.4	15–25
Net Benefit (CAD)	307.5	361.2	412.4	459.9	316.8	370.4	421.7	469.5	-

3. Load Optimization Using the Proposed ML Model

This work integrates empirical data, computational modeling, and ML techniques to analyze key parameters such as efficiency, accuracy, and cost that affect SGBs. The goal is to optimize load consumption in SGTs and improve sustainability [49–52]. The proposed hybrid model predicts load consumption and optimizes HVAC and lighting systems, as well as electricity usage. It combines the spatial feature extraction of CNNs with the temporal learning of LSTM. It is trained using historical data [49]. The optimization framework focuses on reducing costs and emissions, improving system performance, and maximizing REI and smart technology for efficient, sustainable operation.

Hybrid models have been shown to outperform traditional ML methods [12,51]. The CNN–LSTM–AE model developed in [51] achieved lower Mean Square Error (MSE), Mean Absolute Error (MAE), Root Mean Squared Error (RMSE), and Mean Absolute Percentage Error (MAPE) compared to other models using datasets from UC Irvine and Korean commercial buildings. In [52], a CNN–LSTM model was used to improve indoor temperature modeling for HVAC control. The performance was better than MLP and LSTM models over multiple time horizons (1–120 min). The proposed model combines a CNN with LSTM to provide effective load optimization in SGTs as well as insights into energy dynamics and performance.

The proposed algorithm for managing SGT energy in island mode employs a deep hybrid model that integrates CNN and LSTM networks [53–55]. Figure 2 presents a flowchart of the algorithm. It involves data analysis, load and energy optimization, SB controls, RE integration, occupant behavior modeling, and continuous monitoring. The algorithm begins with data input, such as load consumption and user behavior, and this is processed using the model.

K-fold cross-validation is employed to train and validate the model [56]. LSTM layers with attention focused on important time-series data, while CNN layers with skip connections extract features from spatial and sequential data. The outputs are integrated to improve prediction accuracy. The algorithm includes two decision nodes. If Condition 1 is met, load optimization is conducted; otherwise, the results are output. Condition 2 determines if RE integration and/or occupant behavior are modeled. The algorithm produces final predictions to optimize energy performance and load efficiency in CSGTs.

Optimization Problem

The optimization problem is multi-objective. It aims to reduce costs and emissions while improving performance [57]. The focus is minimizing total energy usage and increasing the integration of RESs and smart technologies. The deep ML model predicts load consumption and optimizes system parameters [58,59]. The objective function is

$$\text{F} = \text{Minimize Total Energy Consumption} - \alpha \times \text{REI} - \beta \times \text{STUI} \tag{29}$$

where the coefficients α and β are based on historical data and prioritize the two key objectives. The values chosen are $\alpha = 0.3$ to emphasize cost minimization and $\beta = 0.2$ to focus on emission reduction with lower priority. This combines load consumption, REI, and STUI into a single function.

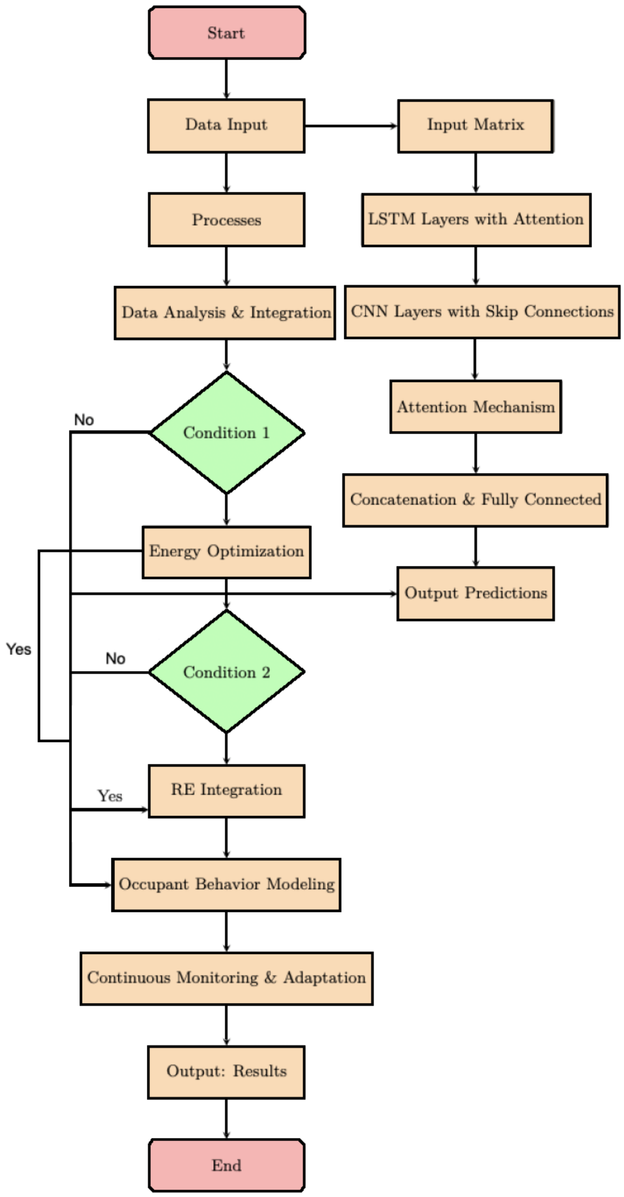

Figure 2. The proposed algorithm flowchart.

The following constraints are used to ensure solutions meet practical and regulatory standards

$$0 \leq \text{TEUI} \leq \text{TEUI}_{\text{max}} \tag{30}$$

$$0 \leq \text{TEDI} \leq \text{TEDI}_{\text{max}} \tag{31}$$

$$0 \leq \text{REI} \leq 100\% \tag{32}$$

$$0 \leq \text{STUI} \leq 100\% \tag{33}$$

$$\text{Energy In} - \text{Energy Out} = \text{Energy Storage} \tag{34}$$

$$\text{Energy Storage}_{\text{min}} \leq \text{Energy Storage} \leq \text{Energy Storage}_{\text{max}} \tag{35}$$

where Energy In includes energy generated from local sources like PV panels, while Energy Out is all energy consumed in the building. Energy Storage is the excess energy stored in batteries. Several variables have minimum or maximum values that restrict possible solutions. For example, thermostat settings are limited to 18–25 °C. According to IEC 62933 [60], the minimum energy storage should be 10% and the maximum should be

90% of total capacity. Constraints, including budget and regulatory requirements, ensure that solutions are realistic and effective.

ML techniques have been used to predict load consumption, optimize resources, and improve sustainability in SGTs and CSGTs. Artificial Neural Networks (ANNs) are effective for load optimization, demand prediction, and anomaly detection. They have also been employed for occupancy forecasting and load anomaly detection using methods such as Holt–Winters–Taylor smoothing and Autoregressive Moving Average (ARMA).

The predicted load is

$$\hat{Y}_t = f(X_t, X_{t-1}, \ldots, X_{t-n}) \tag{36}$$

where $X_t, X_{t-1}, \ldots, X_{t-n}$ are the historical load data and other relevant features, and f is the prediction function. The predicted occupancy is

$$\hat{O}_t = g(T_t, D_t, W_t, O_{t-1}, \ldots, O_{t-n}) \tag{37}$$

where T_t, D_t, and W_t are the time, day, and weather features, and $O_{t-1}, \ldots, O_{t-n}$ are the historical occupancy data.

The goal for HVAC optimization is to minimize load consumption while meeting comfort constraints

$$\min_u \sum_t C_t(u_t) \tag{38}$$

where u_t is the control input at time t and $C_t(u_t)$ is the corresponding load consumption cost. Comfort and operational constraints keep the system within acceptable limits. Comfort constraints ensure thermal comfort by penalizing deviations from desired temperature or humidity set-points. HVAC behavior over time is dynamic as it responds to inputs and disturbances. It can be modeled using physics-based equations or simulation and ML models like LSTM can capture these dynamics.

The integration of LSTM and CNN layers enables the model to capture temporal dependencies and spatial patterns. Attention mechanisms focus on the most relevant features while skip connections improve feature representation and generalization. This architecture can adapt to varying input conditions and handle sequences of different lengths and complexities while mitigating the vanishing gradient problem and ensuring fast convergence. The proposed model has three LSTM layers and three CNN layers. The outputs of these layers are concatenated to fuse temporal and spatial representations. The combined features are passed through a fully connected layer to reduce the dimensionality and refine the data for prediction. The final output layer provides the predictions.

Figure 3 gives the data processing flowchart. The input data are normalized using scaling and are preprocessed for cleaning, missing value imputation, and handling outliers. The data are then split into training, testing, and validation sets. Non-cyclic features (e.g., time components) and correlated attributes are used to improve prediction accuracy. The data are normalized between 0 and 1 using min–max normalization

$$L_{t\mathrm{norm}} = \frac{L_t - L_{\min}}{L_{\max} - L_{\min}} \tag{39}$$

where L_t is the tth original value at time t, and $L_{\max}$ and the $L_{\min}$ are the maximum and minimum values, respectively. The resulting feature vectors have the form

$$X = [L, H, D, M, Ho, Wp, Sp, SUp, Apg] \tag{40}$$

where L is the past load values, H is the hour of the day (time-based variations), D is the day of the week (daily usage patterns), M is the month (seasonal changes), Ho is a holiday indicator (binary/categorical), Wp encompasses weather parameters such as temperature and humidity, Sp is the spatial features (e.g., building size and occupancy), SUp is usage patterns such as peak usage times, and Apg is the appliance usage data. These nine features are the input to the ML model.

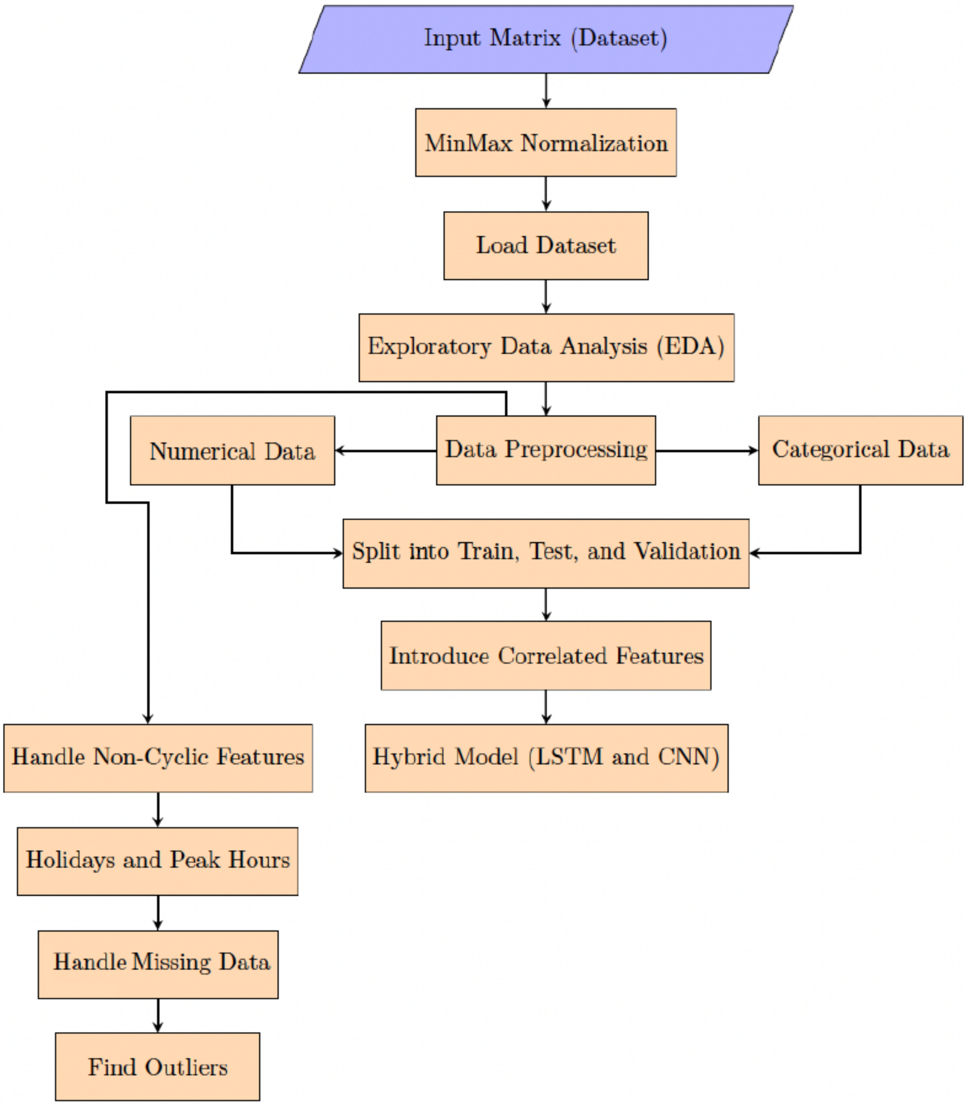

Figure 3. The data processing flowchart [61].

4. Performance Results

Building data, including system architecture, load consumption, and weather conditions, were collected for the SGTs to ensure adaptability to different conditions. OpenStudio was used to simulate energy use and Python libraries (pandas [62], NumPy [63], and Matplotlib [64]), were employed to analyze and visualize the data. Ninja [65] was employed to compare PV systems. Historical datasets such as AMPds2 [21–23,31] were used to train and validate the ML models. Island mode in Burnaby assumes CSGTs disconnected from the BC Hydro grid, so energy from PV panels and EVs must be used. This reduces GHG emissions and electricity costs and improves resilience by satisfying household energy needs while selling surplus energy.

Figure 4 presents the monthly electricity consumption for one- to four-bedroom SGTs and CSGTs in island mode (2012–2014). This shows that both SGTs and CSGTs have higher electricity consumption in the winter due to greater heating demands. However, CSGTs consume more electricity than SGTs, particularly in larger units (3-Bd and 4-Bd), indicating that smart features contribute to increased loads. Thus, while CSGTs provide advanced functionalities, these result in greater energy demands.

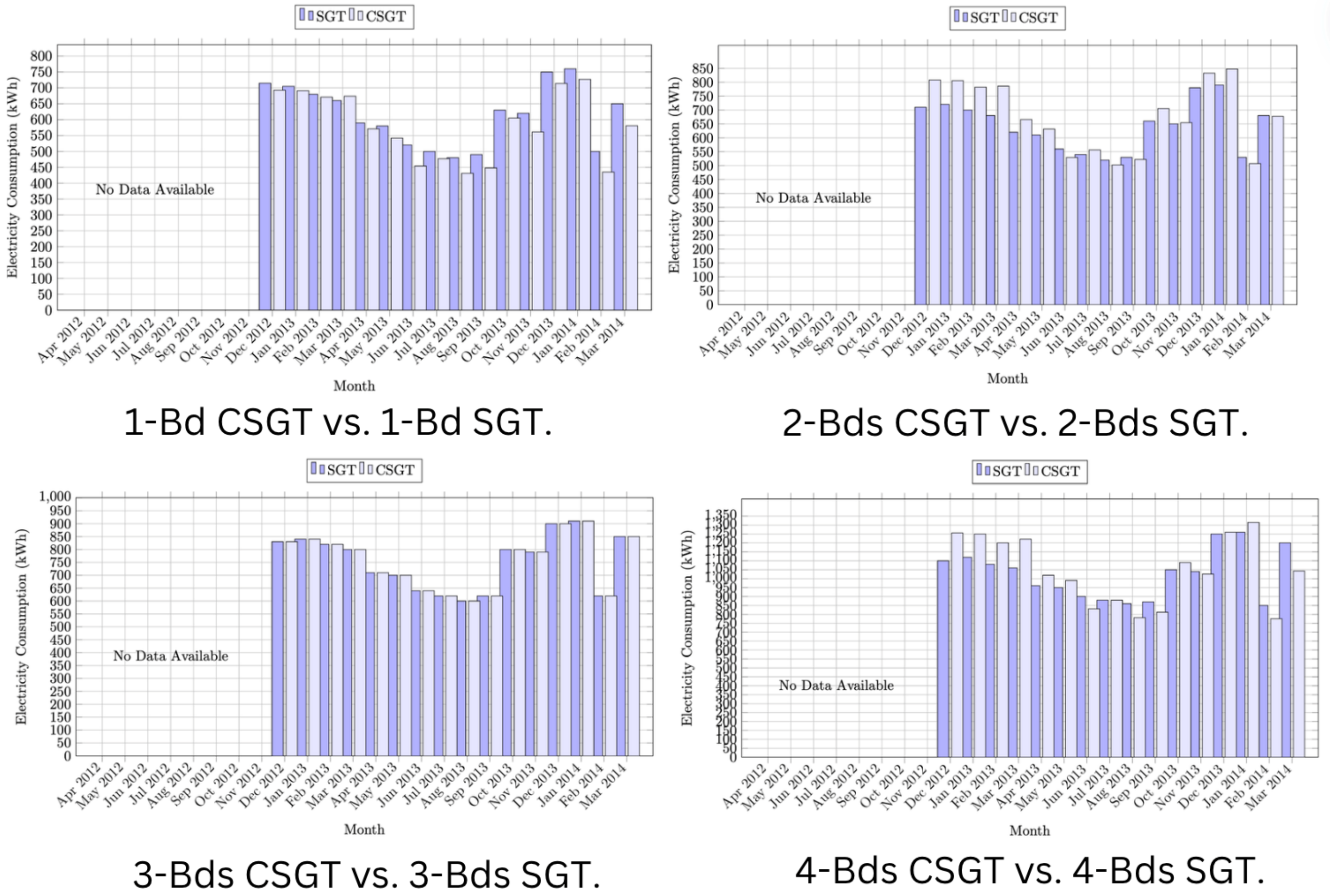

Figure 4. Monthly electricity consumption for one- to four-bedroom SGTs and CSGTs in island mode (2012–2014).

4.1. Impact of Island Mode on Gas and Water Consumption

Island mode operation significantly impacts gas and water consumption in SGTs, as buildings operate independently from the grid. In cold climates like Canada, gas consumption increases in island mode to meet heating needs, especially when it is used for heating. SGT energy management systems can balance gas and electricity energy use in island mode to ensure a consistent energy supply without over-reliance on a single source.

In island mode, SGTs may shift from electric to gas water heating to manage electricity constraints while ensuring hot water availability [66,67]. Water-efficient systems have stricter water-use policies, reduced irrigation, and occupant-driven conservation behavior [67]. The Urban Heat Island (UHI) influence on building load consumption [68] provides important information for optimizing resource use [69]. These results emphasize the need for energy management and resource optimization to maintain sustainability in off-grid conditions.

In island mode, PV panels and EVs significantly reduce gas reliance by generating and storing renewable energy, particularly for 3-Bd and 4-Bd units. The Tesla Model 3 batteries store excess solar energy to power electric heating systems and reduce gas use. Figure 5 shows higher winter gas consumption for heating, with SGTs consuming more gas than CSGTs. This highlights the efficiency of CSGTs in managing loads, especially in larger units, supported by optimized systems and PV panel integration.

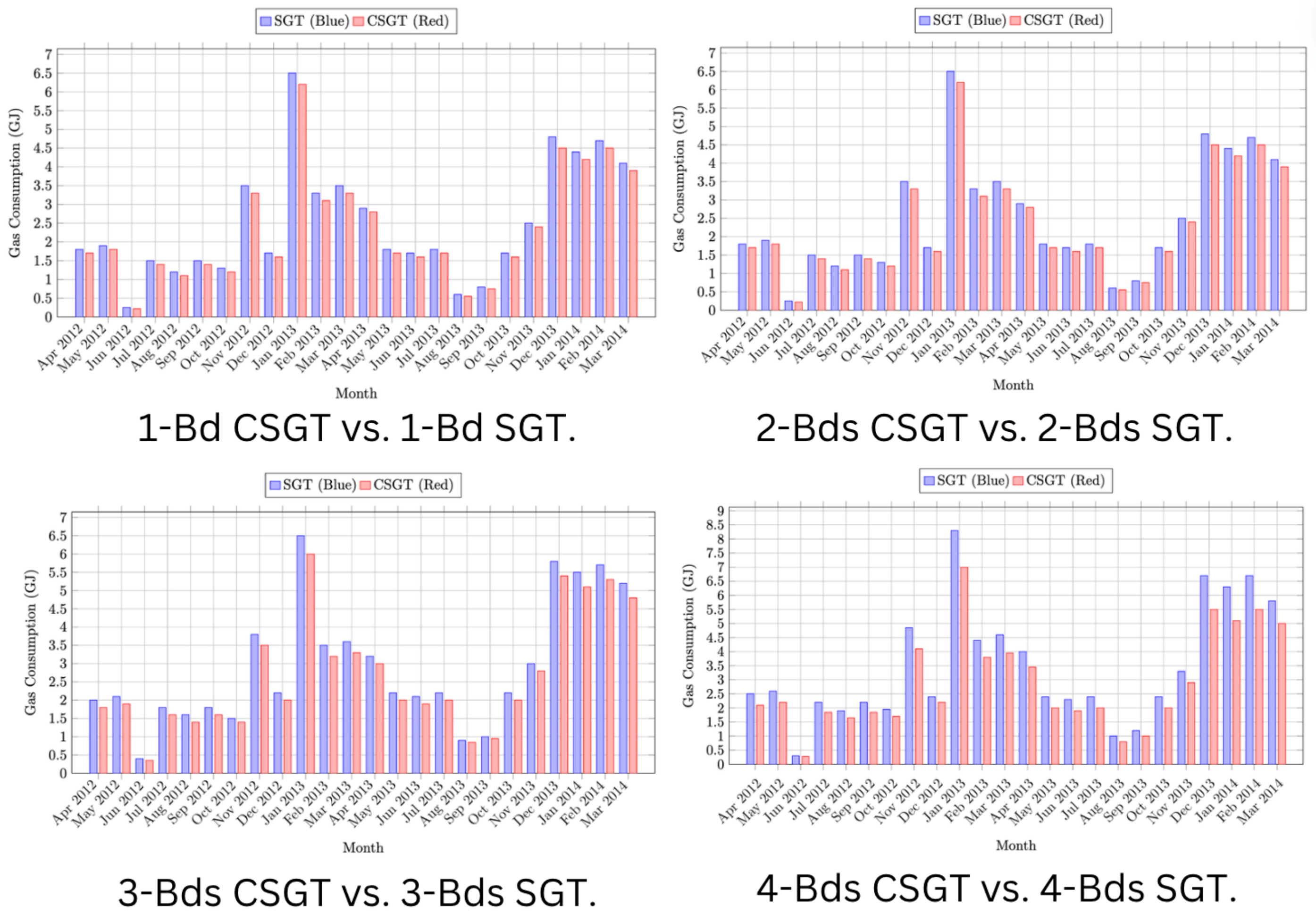

Figure 5. Monthly gas consumption for one- to four-Bd SGTs and CSGTs in island mode (2012–2014).

Figure 6 presents the water consumption for January to December 2013 in island mode, split into indoor (bathing, cooking, laundry) and outdoor (lawn watering) use. CSGTs show lower total water consumption than SGTs, with a 12.5% reduction for all unit sizes. In July 2013, CSGTs used 400–1000 L less water, with a savings of 950 L for 1-Bd units. Peak consumption was reduced by 15% in July 2013, and yearly water consumption was 10,000 L less per unit, reflecting sustainable design. CSGTs also have 10–20% lower water use due to water-conscious behavior through smart systems. Overall, CSGTs in island mode save 14.8% more water than SGTs, with 4-bedroom units saving around 11,000 L yearly.

In island mode, thermal comfort zones (cold, cool, comfortable, warm, too warm) remain consistent across townhouse sizes, suggesting good design principles. The comfortable zone, defined as 20–23 °C, 40–60% humidity, and 0.3–0.5 m/s airflow, aligns with general comfort preferences, ensuring optimal conditions in CSGTs. PV panels and a Tesla Model 3 EV improve sustainability and load efficiency, supporting thermal comfort. Airflow increases from 0.1–0.2 m/s in the cold zone to above 0.7 m/s in the warm zone, ensuring adequate ventilation. Data from the Ninja website support these results [65].

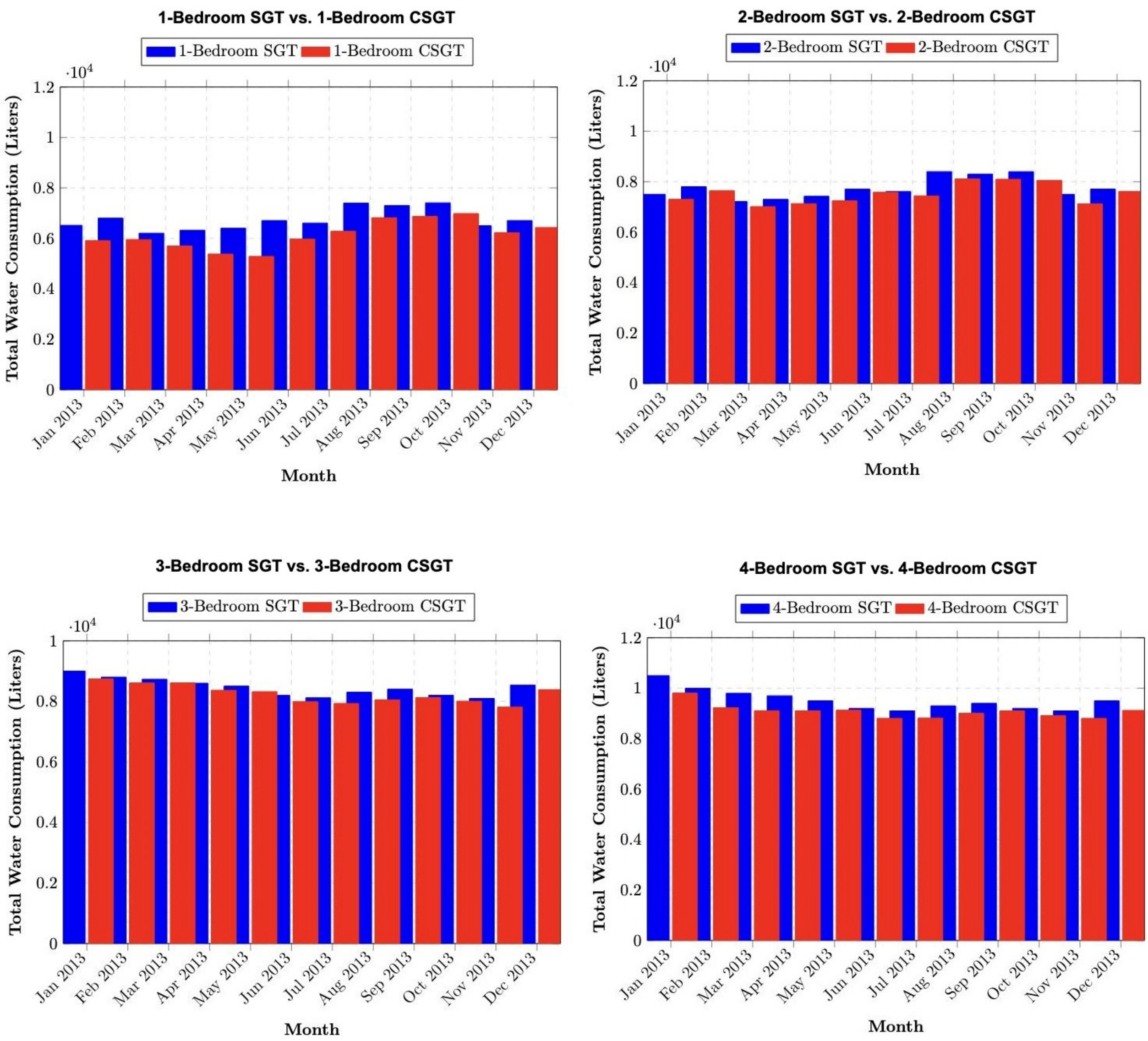

Figure 6. Monthly water consumption for one- to four-Bd SGTs and CSGTs for January to December 2013 in island mode.

4.2. ML Model Results

A hybrid LSTM–CNN model tailored for energy prediction is employed [36]. The proposed model is evaluated along with several well-known models, including LR, LSTM, CNN, RF, Gradient Boosting (GB), and hybrid LSTM–CNN, to assess their performance in SGBs. LR serves as a simple baseline, LSTM excels in handling sequential data, CNN is good at recognizing spatial patterns, RF is robust at managing non-linear relationships and noisy data, GB improves accuracy through ensemble learning, and hybrid LSTM–CNN captures both temporal and spatial dependencies. RF, which utilizes decision tree ensembles, is included to provide a contrast to the deep learning approaches.

Figures 7–10 present the CSGT electricity consumption prediction results for 1- to 4-Bd CSGTs in island mode with the LR, CNN, LSTM, RF, hybrid LSTM–CNN, GB, and proposed ML models. CSGT (red line) is actual consumption, while the other lines show model predictions. These results indicate that, as the number of bedrooms increases, consumption also increases due to larger spaces and higher energy needs. The proposed model provides the best consumption predictions that closely match the actual data. This is because its complex architecture handles data variability better than the other models, making it effective for optimizing energy use and reducing costs in SGTs.

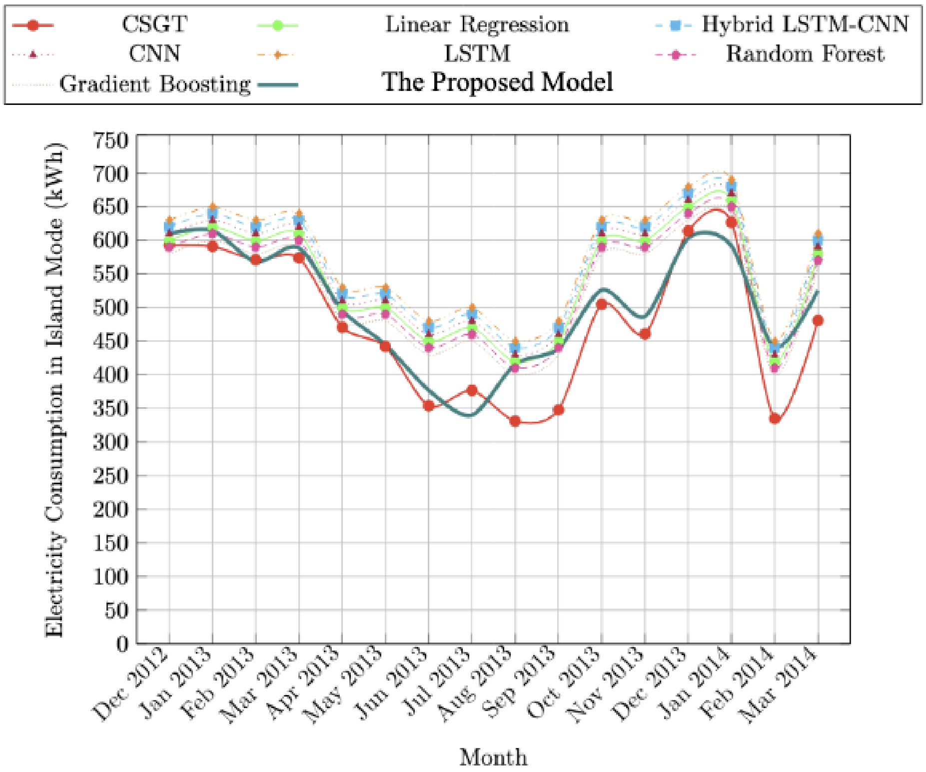

Figure 7. Actual versus predicted monthly electricity consumption with 7 ML models for a one-Bd CSGT in island mode (2012–2014).

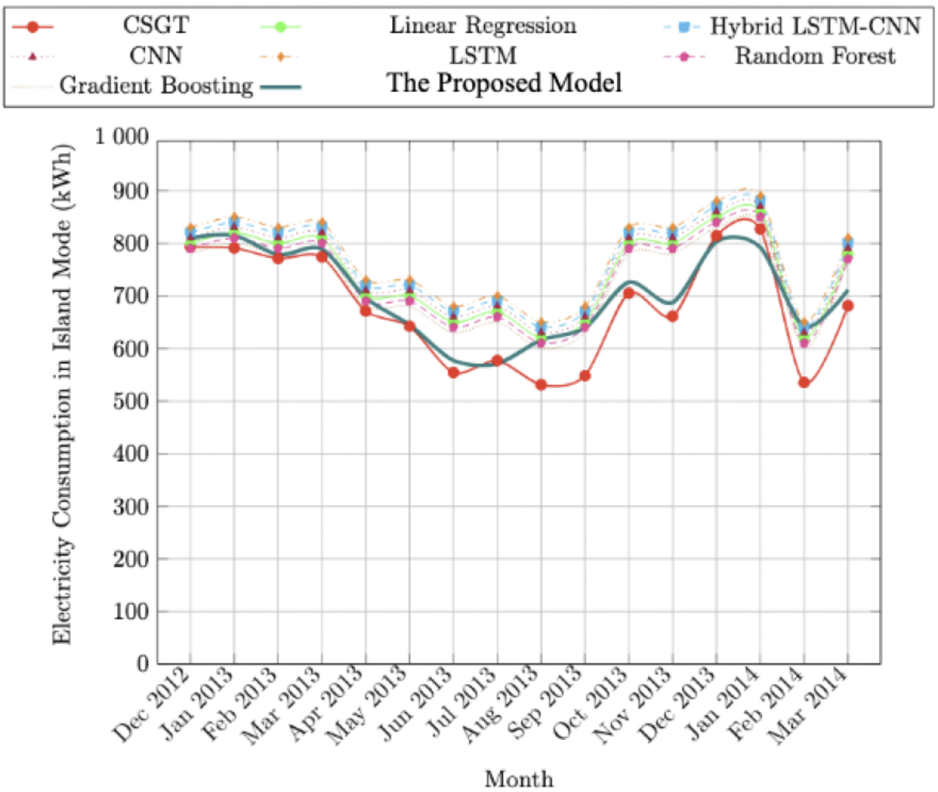

Figure 8. Actual versus predicted monthly electricity consumption with 7 ML models for a two-Bd CSGT in island mode (2012–2014).

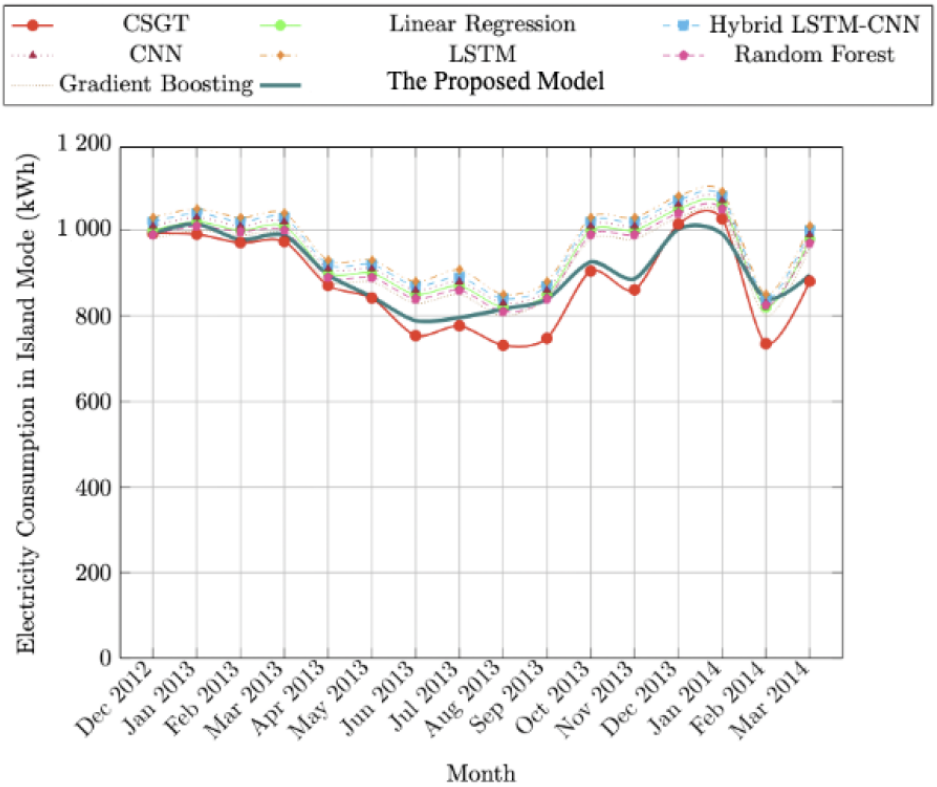

Figure 9. Actual versus predicted monthly electricity consumption with 7 ML models for a three-Bd CSGT in island mode (2012–2014).

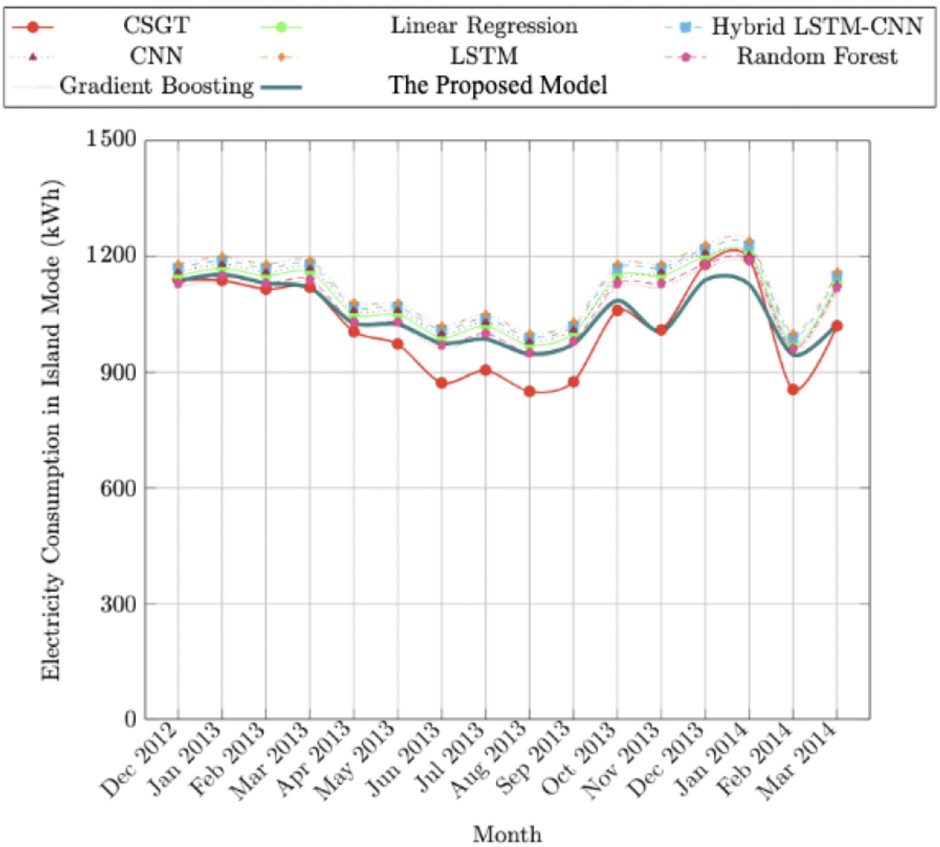

Figure 10. Actual versus predicted monthly electricity consumption with 7 ML models for a four-Bd CSGT in island mode (2012–2014).

Table 6 presents the performance of connected and disconnected SGTs with 1 to 4 bedrooms in island mode, with and without the proposed ML model. The acceptable ranges are MAPE < 10% (very good), 10–20% (acceptable); RMSE < 10% of data range; MAE < 5–10% of mean value; $R^2 > 0.8$ (acceptable), > 0.9 (very good). The data range and mean consumption are as follows: 1-Bd (280 kWh, 600 kWh), 2-Bd (350 kWh, 800 kWh), 3-Bd (400 kWh, 1000 kWh), 4-Bd (500 kWh, 1150 kWh). These results fall within the acceptable range, indicating that the model is effective. The ML model improves the prediction accuracy and thus the efficiency, as the MAPE, RMSE, and MAE are lower. The R^2 values are greater than 0.80 in most cases, demonstrating better performance than without the ML model.

Table 6. Monthly energy performance for SGTs and CSGTs with and without the proposed ML model.

Parameter	Without the ML Model								With the ML Model							
	Connected SGTs				Disconnected SGTs				Connected SGTs				Disconnected SGTs			
	1-Bd	2-Bd	3-Bd	4-Bd	1-Bd	2-Bd	3-Bd	4-Bd	1-Bd	2-Bd	3-Bd	4-Bd	1-Bd	2-Bd	3-Bd	4-Bd
MAPE (%)	3.82	4.15	4.57	5.02	3.91	4.25	4.68	5.12	2.68	3.48	3.61	4.43	2.73	3.51	3.64	4.48
RMSE (kWh)	2.88	3.35	3.76	4.25	2.97	3.42	3.83	4.32	2.03	2.63	2.93	3.49	2.09	2.72	2.98	3.56
MAE (kWh)	2.31	2.74	3.23	3.68	2.38	2.81	3.28	3.75	1.83	1.98	2.78	3.06	1.89	2.04	2.85	3.17
R^2	0.86	0.81	0.77	0.72	0.85	0.80	0.75	0.72	0.98	0.91	0.85	0.81	0.93	0.88	0.81	0.76

Table 7 presents the parameters and performance of the 7 ML models, including the number of layers, neurons, training iterations per epoch, training time per epoch, accuracy, and MAE. This shows that the proposed model achieves the highest accuracy (95%) and a low MAE (0.013), but with the highest computational cost in terms of training time and number of iterations. The hybrid LSTM–CNN model also performs well (90% accuracy, MAE of 0.011). The ensemble models RF and GB provide good accuracy (89–90%) and reasonable MAE. LSTM has moderate computational cost and provides good performance (88% accuracy, MAE of 0.015), while CNN (86% accuracy, MAE of 0.018) performs well. LR has low accuracy (84%) and high MAE (0.02) because it is the baseline, but it has low computational cost.

Table 7. Number of layers, neurons, training iterations per epoch, training time per epoch, error, and accuracy for 7 ML models.

Model	Layers	Neurons	Average Training Iterations per Epoch	Average Training Time per Epoch	Accuracy (%)	MAE
LR	N/A	N/A	261	70 s	84%	0.02
LSTM	3	128	233	6 min	88%	0.015
CNN	5	64	324	10 min	86%	0.018
Random Forest	Trees: 100	Trees: 100	1120	5 min	89%	0.016
Gradient Boosting	Trees: 100	Trees: 100	1051	6 min	90%	0.017
Hybrid LSTM-CNN	LSTM: 2, CNN: 3	LSTM: 64, CNN: 64	753	22 min	90%	0.011
Proposed	LSTM: 3, CNN: 3	LSTM: 128, CNN: 128	1012	28 min	95%	0.013

The MAPE and MAE for day-ahead predictions for CSGTs in island mode vary depending on weather, occupancy, and resource consumption behavior. Figure 11 gives the hourly variations in MAPE and MAE for day-ahead predictions for 3 January 2013. This shows that the error fluctuations are between 3.30% and 4.50% and that the MAE ranges from 2.45 kWh to 3.60 kWh. Both metrics decrease throughout the day, indicating improved prediction accuracy. Considering that island mode can be expected to have greater errors compared to grid-connected mode, the proposed model provides excellent results.

The normality and homoscedasticity residuals [70,71] are used to validate model performance. They represent the differences between actual and predicted values, which range from −2 kWh to 1 kWh. The normality (Shapiro–Wilk test) residual has a p-value of 0.061, which is greater than the standard threshold of 0.05. Thus, it conforms to a normal distribution with random deviations from the mean. The homoscedasticity (Breusch–Pagan test) residual has a p-value of 0.076. This shows that the variance is consistent. These results indicate that the model predictions are reliable.

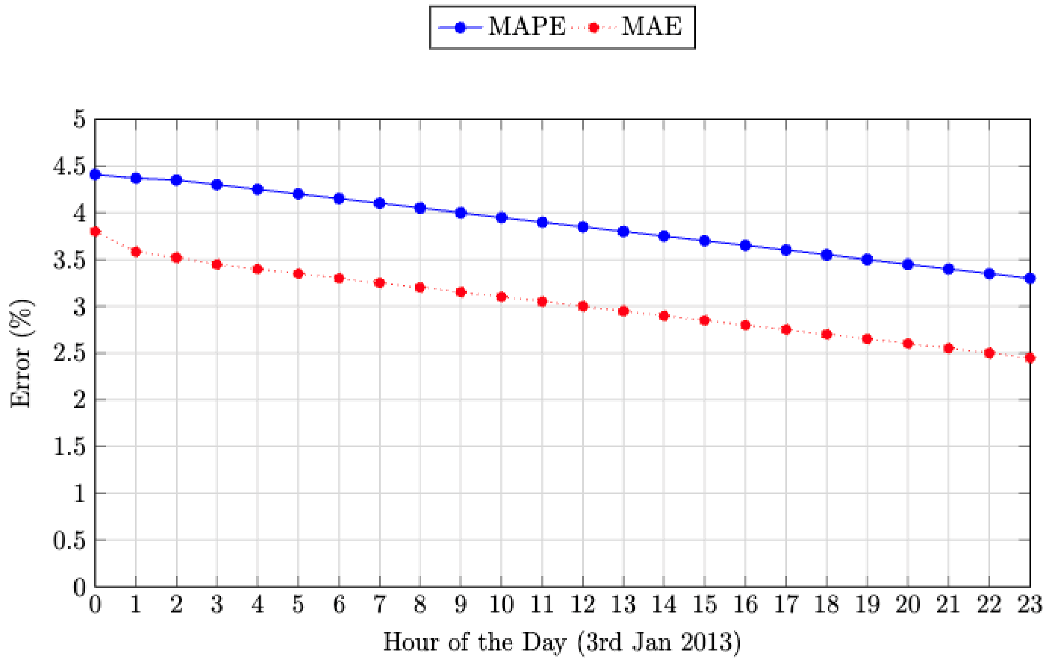

Figure 11. Hourly one-day-ahead prediction of MAPE and MAE for 3 January 2013.

5. Conclusions

Connected Smart Green Townhouses (CSGTs) in island mode were considered to improve energy efficiency by integrating Renewable Energy Sources (RESs) such as PV panels and energy-efficient HVAC systems. The goal was to reduce load consumption, Greenhouse Gas (GHG) emissions, and reliance on fossil fuels while promoting sustainability. Operating independently of the grid, island mode offers resilience during outages and optimizes local energy storage and utilization, minimizing the carbon footprint.

The proposed ML model was developed to predict energy system performance by capturing temporal and spatial dependencies in energy data. Energy management was optimized for connected and disconnected Smart Green Townhouses (SGTs) to reduce energy waste and costs. A Mean Absolute Percentage Error (MAPE) of 3.30–4.50% and a Mean Absolute Error (MAE) of 2.45–3.60 kWh for day-ahead predictions were achieved, indicating excellent accuracy to support sustainable urban development.

In the future, parameter tuning can be considered to improve model performance. Occupant behavior can also be incorporated into real-time energy policies. The goal is to improve energy utilization, minimize waste, and foster sustainable practices in urban living.

Author Contributions: Conception and design, S.M.M., T.A.G., I.T.C. and H.T.; preparation and analysis, S.M.M., I.T.C. and T.A.G.; writing—original draft, T.A.G., S.M.M. and I.T.C.; writing—review and editing, T.A.G., S.M.M., I.T.C. and H.T.; supervision, T.A.G. All authors have read and agreed to the published version of the manuscript.

Funding: This research received no external funding.

Data Availability Statement: The original contributions presented in the study are included in the article; further inquiries can be directed to the corresponding author.

Conflicts of Interest: The authors declare no conflicts of interest.

Abbreviations

The following abbreviations are used in this manuscript.

Symbol	Description	Symbol	Description
ANN	Artificial Neural Network	MAE	Mean Absolute Error
BC	British Columbia	MAPE	Mean Absolute Percentage Error
BMS	Building Management System	MG	Micro-Grid
CAD	Canadian Dollar	ML	Machine Learning
CEI	Control Efficiency Index	MRP	Material Recycling Percentage
CGBC	Canada Green Building Council	MSE	Mean Square Error
CNN	Convolutional Neural Network	NN	Neural Network
COP	Coefficient of Performance	PV	Photovoltaic
CSGTs	Connected Smart Green Townhouses	REI	Renewable Energy Integration
EDA	Exploratory Data Analysis	RES	Renewable Energy Source
ECE	Electrical Consumption Efficiency	RF	Random Forest
EER	Energy Efficiency Ratio	RMSE	Root Mean Square Error
EV	Electric Vehicle	SB	Smart Building
GCE	Gas Consumption Efficiency	SGB	Smart Green Building
GB	Green Building	SG	Smart Grid
GHG	Greenhouse Gas	SGI	Smart Grid Integration
GHGI	Greenhouse Gas Index	SGT	Smart Green Townhouse
HDD	Heating Degree Days	STUI	Smart Technology Utilization Index
HSPF	Heating Seasonal Performance Factor	TEDI	Total Energy Demand Intensity
HVAC	Heating, Ventilation, and Air Conditioning	TEUI	Total Energy Use Intensity
IAQ	Indoor Air Quality	TWMU	Total Weight of Materials Used
LED	Light Emitting Diode	V2G	Vehicle-to-Grid
LEED	Leadership in Energy and Environmental Design	VOC	Volatile Organic Compound
LR	Linear Regression	WRM	Weight of Recycled Materials
LSTM	Long Short-Term Memory	WRR	Waste Recycling Rate
		WRW	Weight of Recycled Waste

References

1. EIA. *Monthly Energy Review—June 2020*; U.S. Energy Information Administration: Washington, DC, USA, 2020. Available online: https://www.eia.gov/totalenergy/data/monthly/archive/00352006.pdf (accessed on 1 January 2024).
2. Hatamian, M.; Panigrahi, B.; Dehury, C.K. Location-aware green energy availability forecasting for multiple time frames in smart buildings: The case of Estonia. *Meas. Sens.* **2023**, *25*, 100644. [CrossRef]
3. Rameshwar, R.; Solanki, A.; Nayyar, A.; Mahapatra, B. Green and smart buildings: A key to sustainable global solutions. In *Green Building Management and Smart Automation*; IGI Global Scientific Publishing: Hershey, PA, USA, 2020. [CrossRef]
4. Mariano-Hernández, D.; Hernández-Callejo, L.; Zorita-Lamadrid, A.; Duque-Pérez, O.; García, F.S. A review of strategies for building energy management system: Model predictive control, demand side management, optimization, and fault detect & diagnosis. *J. Build. Eng.* **2021**, *33*, 101692. [CrossRef]
5. Ngo, N.T.; Pham, A.D.; Truong, T.T.H.; Truong, N.S.; Huynh, N.T.; Pham, T.M. An ensemble machine learning model for enhancing the prediction accuracy of energy consumption in buildings. *Arab. J. Sci. Eng.* **2022**, *47*. [CrossRef]
6. Liu, X.; Wang, Z.; Zheng, R. An ensemble learning framework for building energy consumption forecasting. *Appl. Energy* **2020**, *262*, 114561. [CrossRef]
7. Nivethitha, S. Gauthama, R. Krithi, R. A hybrid model for building energy demand forecasting using long short-term memory and convolutional neural network. *Appl. Energy* **2019**, *261*, 114131. [CrossRef]
8. Sunder, R.; Sreeraj, R.; Vince, P.; Sanjeev, K. P.; Bhagavan, K.; Konduri, B.; Nabilal, K.V.; Lilhore, U.K.; Ghith, T. K.L.E.; Tlija, M. An advanced hybrid deep learning model for accurate energy load prediction in smart building. *Energy Explor. Exploit.* **2024**, *42*, 2241–2269. [CrossRef]
9. Daorui, D.; Chang, H.; Kumar, B.V.D. Optimized energy distribution in smart grid system using hybrid machine learning techniques. In Proceedings of the IEEE International Conference on Software Engineering and Computer Systems, Penang, Malaysia, 25–27 August 2023. [CrossRef]
10. Islam, M.T.; Ayon, E.H.; Ghosh, B.P.; Shahid, R.; Rahman, S.; Bhuiyan, M.S.; Nguyen, T.N. Revolutionizing retail: A hybrid machine learning approach for precision demand forecasting and strategic decision-making in global commerce. *J. Comput. Sci. Technol. Stud.* **2024**, *6*, 33–39. [CrossRef]
11. Kim, S.; Lim, H. Reinforcement learning based energy management algorithm for smart energy buildings. *Energies* **2018**, *11*, 2010. [CrossRef]
12. Parizad, B.; Ranjbarzadeh, H.; Jamali, A.; Khayyam, H. An intelligent hybrid machine learning model for sustainable forecasting of home energy demand and electricity price. *Sustainability* **2024**, *16*, 2328. [CrossRef]

13. Nasruddin, S.; Satrio, P.; Mahlia, T.M.I.; Giannetti, N.; Saito, K. Optimization of HVAC system energy consumption in a building using artificial neural network and multi-objective genetic algorithm. *Sustain. Energy Technol. Assess.* **2019**, *33*, 48–57. [CrossRef]
14. Al-Rakhami, M.; Gumaei, A.; Alsanad, A.; Alamri, A.; Hassan, M.M. An ensemble learning approach for accurate energy load prediction in residential buildings. *IEEE Access* **2019**, *7*, 48328–48338. [CrossRef]
15. Vandenberg, V. Greener Small Cities: Deploy Environmental Action Faster and Smarter. Masters Thesis, OCAD University, Toronto, ON, Canada, 2022. Available online: https://openresearch.ocadu.ca/id/eprint/3558/1/Vandenberg_Victoria_2021_MDES_SFI_MRP.pdf (accessed on 1 January 2024).
16. Condon, F.; Martínez, J.M.; Eltamaly, A.M.; Kim, Y.C.; Ahmed, M.A. Design and implementation of a cloud-IoT-based home energy management system. *Sensors* **2022**, *23*, 176. [CrossRef]
17. Bahmanyar, D.; Razmjooy, N.; Mirjalili, S. Multi-objective scheduling of IoT-enabled smart homes for energy management based on arithmetic optimization algorithm: A Node-RED and NodeMCU module-based technique. *Knowl.-Based Syst.* **2022**, *247*, 108762. [CrossRef]
18. Zhou, X.; Du, H.; Xue, S.; Ma, Z. Recent advances in data mining and machine learning for enhanced building energy management. Sustainable cities and society. *Energy* **2024**, *307*, 132636. [CrossRef]
19. Berardi, U.; Jafarpur, P. Assessing the impact of climate change on building heating and cooling energy demand in Canada. *Renew. Sustain. Energy Rev.* **2020**, *121*, 109681. [CrossRef]
20. Sultana, J.; Singha, A.K.; Siddiqui, S.T.; Nagalaxmi, G.; Sriram, A.K.; Pathak, N. COVID-19 pandemic prediction and forecasting using machine learning classifiers. *Intell. Autom. Soft Comput.* **2022**, *32*, 1007–1024. [CrossRef]
21. Makonin, S. Ellert, B. Bajić, I.V. Popowich F. Electricity, water, and natural gas consumption of a residential house in Canada from 2012 to 2014. *Sci. Data* **2016**. *3*, 160037. [CrossRef]
22. Makonin, S.; Popowich, F.; Bartram, L.; Gill, B.; Bajić, I.V. AMPds: A public dataset for load disaggregation and eco-feedback research. In Proceedings of the IEEE Electrical Power & Energy Conference, Halifax, NS, Canada, 21–23 August 2013. [CrossRef]
23. Gaur, M.; Makonin, S.; Bajić, I. V.; Majumdar, A. Performance evaluation of techniques for identifying abnormal energy consumption in buildings. *IEEE Access* **2019**, *7*, 62721–62733. [CrossRef]
24. Lin B.; Chen, Z. Net zero energy building evaluation, validation and reflection—A successful project application. *Energy Build.* **2022**, *261*, 111946. [CrossRef]
25. Adier, M.F.V.; Sevilla, M.E.P.; Valerio, D.N.R.; Ongpeng, J.M.C. Bamboo as sustainable building materials: A systematic review of properties, treatment methods, and standards. *Buildings* **2023**, *13*, 2449. [CrossRef]
26. Susanto, D.; Widyarko, W. Sustainable material: Used wood as building material. *Int. Ser. Interdiscip. Sci. Technol.* **2017**, *2*, 14–18. [CrossRef]
27. Yu, B.; Fingrut, A. Sustainable building design (SBD) with reclaimed wood library constructed in collaboration with 3D scanning technology in the UK. *Resour. Conserv. Recycl.* **2022**, *179*, 106566. [CrossRef]
28. Bribián, I.Z.; Capilla, A.V.; Uson, A.A. Life cycle assessment of building materials: Comparative analysis of energy and environmental impacts and evaluation of the eco-efficiency improvement potential. *Build. Environ.* **2011**, *46*, 1133–1140. [CrossRef]
29. Stoikov, V.; Gassiy, V. Energy efficiency of housing as a tool for sustainable development. *MATEC Web Conf.* **2018**, *251*, 03061. [CrossRef]
30. Gado, A.; Ibrahim, M.; Youssef, A. Feasibility of rainwater harvesting for sustainable water management in urban areas of Egypt. *Environ. Sci. Pollut. Res.* **2020**, *27*, 32304–32317. [CrossRef] [PubMed]
31. Decuypere, R.; Robaeyst, B.; Hudders, L.; Baccarne, B.; Van De Sompel, D. Transitioning to energy efficient housing: Drivers and barriers of intermediaries in heat pump technology. *Energy Policy* **2021**, *156*, 112709. [CrossRef]
32. Benavente-Peces, C. On the energy efficiency in the next generation of smart buildings—Supporting technologies and techniques. *Energies* **2019**, *12*, 4399. [CrossRef]
33. Homod, R.Z. Analysis and optimization of HVAC control systems based on energy and performance considerations for smart buildings. *Renew. Energy* **2018**, *126*, 49–64. [CrossRef]
34. Maasoumy, M.; Sangiovanni-Vincentelli, A. Smart connected buildings design automation: Foundations and trends. *Found. Trends Electron. Des. Autom.* **2016**, *12*, 156. [CrossRef]
35. Lawton, M.; Roppel, P.; Fookes, D.; Teasdale St. Hilaire, A.; Schoonhoven, D. Real R-value of exterior insulated wall assemblies. In Proceedings of the Building Enclosure Science and Technology Conference, Portland, OR, USA, 12–14 April 2010. Available online: https://fs.hubspotusercontent00.net/hubfs/2011056/BuildingScience/White%20Papers/Real%20R-Value%20of%20Exterior%20Insulated%20Wall%20Assemblies.pdf (accessed on 1 January 2024).
36. Sharma, R.; Goel, S. Performance analysis of a 11.2 kWp roof top grid-connected PV system in Eastern India. *Energy Rep.* **2017**, *3*, 103–112. [CrossRef]
37. Duffie, J.A.; Beckman, W.A.; Blair, N. *Solar Engineering of Thermal Processes, Photovoltaics and Wind*; John Wiley & Sons: Hoboken, NJ, USA, 2020. [CrossRef]
38. Thomas, D.; Deblecker, O.; Ioakimidis, C.S. Optimal operation of an energy management system for a grid-connected smart building considering photovoltaics' uncertainty and stochastic electric vehicles' driving schedule. *Appl. Energy* **2017**, *210*. [CrossRef]
39. Moghimi, S.M.; Shariatmadar, S.M.; Dashti, R. Stability analysis of the micro-grid operation in micro-grid mode based on particle swarm optimization (PSO) including model information. *Phys. Sci. Int. J.* **2016**, *10*, PSIJ.24779. [CrossRef]

40. Amir, V.; Jadid, S.; Ehsan, M. Operation of networked multi-carrier microgrid considering demand response. *Compel Int. J. Comput. Math. Electr. Electron. Eng.* **2019**, *38*, 724–744. . [CrossRef]
41. Jangsten, M.; Lindholm, T.; Dalenbäck, J.O. Analysis of operational data from a district cooling system and its connected buildings. *Energy* **2020**, *203*, 117844. [CrossRef]
42. Agugiaro, G.; Zwamborn, A.; Tigchelaar, C.; Matthijssen, E.; León-Sánchez, C.; Van Der Molen, F.; Stoter, J. On the influence of party walls for urban energy modelling. *Int. Arch. Photogramm. Remote Sens. Spatial Inf. Sci.* **2022**, *XLVIII-4/W5-2022*, 9–16. [CrossRef]
43. Palmer, J.; Terry, N. Looking critically at heat loss through party walls. *Sustainability* **2022**, *14*, 3072. [CrossRef]
44. Kim, D.; Yoon, Y.; Lee, J.; Mago, P.J.; Lee, K.; Cho, H. Design and implementation of smart buildings: A review of current research trends. *Energies* **2022**, *15*, 4278. [CrossRef]
45. Mariano-Hernández, D.; Hernández-Callejo, L.; García, F.S.; Duque-Perez, O.; Zorita-Lamadrid, A.L. A review of energy consumption forecasting in smart buildings: Methods, input variables, forecasting horizon and metrics. *Appl. Sci.* **2020**, *10*, 8323. [CrossRef]
46. Goetzler, W.; Guernsey, M.; Young, J.; Fujrman, J.; Abdelaziz, A. *The Future of Air Conditioning for Buildings (No. DOE/EE-1394)*; Navigant Consulting: Burlington, MA, USA, 2016. [CrossRef]
47. Chan, J.; Frisque, A.; Jang, A. Designing to TEDI, TEUI, and GHGI performance metrics. In Proceedings of the IBPSA International Conference, Rome, Italy, 2–4 September 2019 . Available online: https://publications.ibpsa.org/proceedings/bs/2019/papers/BS2019_211370.pdf. (accessed on 1 January 2024).
48. Janhunen, E. Is Smart Profitable for Real Estate?-Evaluating the Viability of Smart Energy Management System Investments for Real Estate Owners. Ph.D. Thesis, Aalto University, Espoo, Finland, 2023. Available online: https://aaltodoc.aalto.fi/items/4a1be465-372a-4711-a1fe-82c220ad79cb (accessed on 20 December 2024).
49. Saxena, H.; Aponte, O.; McConky, K.T. A hybrid machine learning model for forecasting a billing period's peak electric load days. *Int. J. Forecast.* **2019**, *35*, 1288–1303. [CrossRef]
50. Lu, C.; Li, S.; Gu, J.; Lu, W.; Olofsson, T.; Ma, J. A hybrid ensemble learning framework for zero-energy potential prediction of photovoltaic direct-driven air conditioners. *J. Build. Eng.* **2023**, *64*, 105602. [CrossRef]
51. Khan, Z.A.; Hussain, T.; Ullah, A.; Rho, S.; Lee, M.; Baik, S.W. Towards efficient electricity forecasting in residential and commercial buildings: A novel hybrid CNN with a LSTM-AE based framework. *Sensors* **2020**, *20*, 1399. [CrossRef] [PubMed]
52. Elmaz, F.; Eyckerman, R.; Casteels, W.; Latré, S.; Hellinckx, P. CNN-LSTM architecture for predictive indoor temperature modeling. *Build. Environ.* **2021**, *206*, 108327. [CrossRef]
53. Ullah, I.; Hasanat, S.M.; Aurangzeb, K.; Alhussein, M.; Rizwan, M.; Anwar, M.S. Multi-horizon short-term load forecasting using hybrid of LSTM and modified split convolution. *Peer J. Comput. Sci.* **2023**, *9*, e1487. [CrossRef]
54. Arora, S.; Taylor, J.W. Short-term forecasting of anomalous load using rule-based triple seasonal methods. *IEEE Trans. Power Syst.* **2013**, *28*, 3235–3242. [CrossRef]
55. Vaswani, A.; Shazeer, N.; Parmar, N.; Uszkoreit, J.; Jones, L.; Gomez, A.N.; Kaiser, Ł.; Polosukhin, I. Attention is all you need. *Adv. Neural Inf. Process. Syst.* **2017**, *30*, 5998–6008. [CrossRef].
56. Halbouni, A.; Gunawan, T.S.; Habaebi, M.H.; Halbouni, M.; Kartiwi, M.; Ahmad, R. CNN-LSTM: Hybrid deep neural network for network intrusion detection system. *IEEE Access* **2022**, *10*, 99837–99849. [CrossRef]
57. Yi, L.; Zhang, H.; Wang, Y.; Luo, B.; Fan, L.; Liu, J.; Hua Li, G. Multi-objective global dynamic optimal scheduling of smart building loads considering carbon emissions. *Energy Build.* **2023**, *301*, 113740. [CrossRef]
58. Sendra-Arranz, R.; Gutiérrez, A. A long short-term memory artificial neural network to predict daily HVAC consumption in buildings. *Energy Build.* **2020**, *216*, 109952. [CrossRef]
59. Moghimi, S. M.; Gulliver, T. A.; Chelvan, I. T. Energy management in modern buildings based on demand prediction and machine learning—A review. *Energies* **2024**, *17*, 555. [CrossRef]
60. International Electrotechnical Commission. Electrical Energy Storage (EES) Systems Part 1: Vocabulary. International Electrotechnical Commission, Geneva, Switzerland, 2024. Available online: https://webstore.iec.ch/publication/64642 (accessed on 20 December 2024).
61. Moghimi, S.M.; Gulliver, T.A.; Thirumai Chelvan, I.; Teimoorinia, H. Resource optimization for grid-connected smart green townhouses using deep hybrid machine learning. *Energies* **2024**, *17*, 6201. [CrossRef]
62. Raschka, S.; Patterson, J.; Nolet, C. Machine learning in Python: Main developments and technology trends in data science, machine learning, and artificial intelligence. *Information* **2020**, *11*, 193. [CrossRef]
63. Harris, C.R.; Millman, K.J.; Van Der Walt, S.J.; Gommers, R.; Virtanen, P.; Cournapeau, D.; Wieser, E.; Taylor, J.; Berg, S.; Smith, N.J.; et al. Array programming with NumPy. *Nature* **2020**, *585*, 357–362. [CrossRef]
64. Hunter, J.D. Matplotlib: A 2D graphics environment. *Comput. Sci. Eng.* **2007**, *9*, 90–95. [CrossRef]
65. Pfenninger, S.; Staffell, I. Long-term patterns of European PV output using 30 years of validated hourly reanalysis and satellite data. *Energy* **2016**, *114*, 1251–1265. [CrossRef]
66. Wang, W.C.; Dwijendra, N.K.A.; Sayed, B.T.; Alvarez, J.R.N.; Al-Bahrani, M.; Alviz-Meza, A.; Cárdenas-Escrocia, Y. Internet of things energy consumption optimization in buildings: A step toward sustainability. *Sustainability* **2023**, *15*, 6475. [CrossRef]
67. Hakawati, B.; Mousa, A.; Draidi, F. Smart energy management in residential buildings: The impact of knowledge and behavior. *Sci. Rep.* **2024**, *14*, 1702. [CrossRef] [PubMed]

68. Li, X.; Zhou, Y.; Yu, S.; Jia, G.; Li, H.; Li, W. Urban heat island impacts on building energy consumption: A review of approaches and findings. *Energy* **2019**, *174*, 407–419. [CrossRef]
69. Zheng, G.; Feng, Z.; Jiang, M.; Tan, L.; Wang, Z. Predicting the energy consumption of commercial buildings based on deep forest model and its interpretability. *Buildings* **2023**, *13*, 2162. [CrossRef]
70. Jochmans, K. Heteroscedasticity-robust inference in linear regression models with many covariates. *J. Am. Stat. Assoc.* **2022**, *117*, 538. [CrossRef]
71. Mishra, P.; Pandey, C.M.; Singh, U.; Gupta, A.; Sahu, C.; Keshri, A. Descriptive statistics and normality tests for statistical data. *Ann. Card. Anaesth.* **2019**, *22*, 538. [CrossRef]